http://dx.doi.org/10.5516/NET.07.2013.706

IRRADIATION EFFECTS OF HT-9 MARTENSITIC STEEL

YIREN CHEN
Nuclear Engineering Division, Argonne National Laboratory, Argonne, IL 60439, USA
E-mail : yiren_chen@anl.gov

Received May 21, 2013

High-Cr martensitic steel HT-9 is one of the candidate materials for advanced nuclear energy systems. Thanks to its excellent thermal conductivity and irradiation resistance, ferritic/martensitic steels such as HT-9 are considered for in-core applications of advanced nuclear reactors. The harsh neutron irradiation environments at the reactor core region pose a unique challenge for structural and cladding materials. Microstructural and microchemical changes resulting from displacement damage are anticipated for structural materials after prolonged neutron exposure. Consequently, various irradiation effects on the service performance of in-core materials need to be understood. In this work, the fundamentals of radiation damage and irradiation effects of the HT-9 martensitic steel are reviewed. The objective of this paper is to provide a background introduction of displacement damage, microstructural evolution, and subsequent effects on mechanical properties of the HT-9 martensitic steel under neutron irradiations. Mechanical test results of the irradiated HT-9 steel obtained from previous fast reactor and fusion programs are summarized along with the information of irradiated microstructure. This review can serve as a starting point for additional investigations on the in-core applications of ferritic/martensitic steels in advanced nuclear reactors.

KEYWORDS : High-Cr Martenistic steels, HT-9, Irradiation Effects, Radiation Damage, Irradiation Embrittlement

1. INTRODUCTION

Alloy HT-9 is a 12%-chromium and 1%-molybdenum steel initially developed in Europe for fossil-fired power generation industry.[1] With a nominal composition of Fe-12Cr-1Mo-0.5W-0.5Ni-0.25V-0.2C (in wt%), the HT-9 steel is a high-strength martensitic stainless steel. Owing to its good creep-rupture strength and oxidation resistance, the HT-9 steel has been widely used since 1960s for components of turbines and boilers in fossil-fired power plants.[1] Besides its non-nuclear applications, the HT-9 steel has also become an attractive candidate material for various nuclear energy systems since 1970s. Alloy HT-9 has been considered for both in-core and out-of-core applications of fast breeder reactors, [2,3] and for the first wall and blanket structures of fusion systems.[4,5] The HT-9 steel has also been used successfully in the Fast Flux Test Facility (FFTF) as fuel cladding and ducts.[6] For nuclear energy applications, the HT-9 and other ferritic/martensitic steels have a number of advantages compared with austenitic stainless steels currently used in light water reactors. Typically, ferritic/martensitic steels have high thermal conductivity, low thermal expansion coefficient, good high-temperature strength, and most importantly, very low void swelling rate under neutron irradiations.[7-9] The excellent thermal properties and dimensional stability make the HT-9 steel one of the most promising candidate materials for future advanced nuclear energy systems, which will undoubtedly be operated at much higher temperatures and harsher irradiation environments than the current light water reactors.

Despite various advantages, some serious challenges do exist for the usage of HT-9 in severe irradiation environments. The most critical issue is low-temperature irradiation embrittlement which affects the fracture resistance of ferritic /martensitic steels considerably after neutron irradiations. With a body-centered cubic (bcc) crystal structure, ferritic /martensitic steels undergo a transition from ductile to brittle fracture with decreasing temperature. It has been shown that the ductile-brittle transition temperature (DBTT) increases rapidly with neutron irradiation at temperatures below 0.3 Tm (absolute melting temperature).[9,10] The upper-shelf energy also decreases significantly along with a reduced strain hardening coefficient and higher degree of flow localization in irradiated ferritic/martensitic steels.[11] This irradiation-induced embrittlement is a critical concern for nuclear energy systems where temperature transients are inevitably present during operation. In addition to the low-temperature embrittlement, high-temperature creep property and rupture strength are another important issue for the applications of HT-9 in nuclear energy systems.[12,13] While a wide range of mechanical properties can be obtained through thermal-mechanical treatments, the high-temperature strength of ferritic/martensitic steels relies on the stability of heat treatment microstructures and secondary phases under neutron irradiations at operating

temperatures. Since irradiation-enhanced diffusion and segregation are important factors for the formation and stability of new phases in ferritic/martensitic alloys, irradiation-induced degradations of the high-temperature performance are of critical concern. Unless the hardening phases can be stabilized, the maximum service temperature of HT-9 may be limited for in-core applications. The importance of the high-temperature strength is reflected in the history of the development of ferritic/martensitic steels, which is essentially a continued effort in improving the creep rupture strength and maximum service temperature.[14] More recently, it has been demonstrated that oxide dispersion-strengthened high-Cr steels may be a potential solution for elevated-temperature strength, [9] but the irradiation embrittlement of these materials needs further investigations.

This review will be focused on the irradiation effects of the HT-9 martensitic steel. The current understanding on the radiation damage, irradiation microstructure evaluation and irradiation induced mechanical property changes in HT-9 will be presented. Since many high-Cr steels share common features and have often been studied alongside with HT-9, other high-Cr (9-12% Cr) ferritic/martensitic steels will also be referred occasionally in the discussion.

2. BACKGROUND OF RADIATION DAMAGE

Radiation damage of crystalline materials arises from the interactions between impinging particles (i.e. neutrons, ions and electrons) and lattice atoms. Along the path of an intruding particle, the kinetic energy of the particle dissipates in the host matrix through electron excitations, elastic collisions and inelastic interactions with the target nuclei.[15] When the energy of elastic collisions is sufficiently high, lattice atoms can be displaced from their original sites, giving rise to primary knock-on atoms (PKAs). The PKAs often have energies exceed the lattice displacement threshold (E_d) by many orders of magnitude, and thus can displace a large number of neighboring atoms, forming displacement cascades.[15-17] Consequently, an avalanche of self-interstitials and vacancies (Frenkel pairs) are produced within the displacement cascades. Most of these point defects annihilate quickly in the cooling phase of the displacement cascades. However, due to crystallographic symmetries, atoms at a considerable distance from the core of a cascade can be displaced via focusing, replacement collisions or by propagation as crowdions. Thus, a vacancy rich core surrounded by an interstitial rich shell is formed by the displacement cascade.[10] At irradiation temperatures, the surviving vacancies and interstitials evolve into crystalline defects through point defect aggregation or cascade core collapsing.

To assess the extent of radiation damage, displacements per atom (*dpa*) is often used as a measure of irradiation dose in nuclear materials research. Using *dpa* as a damage-based exposure unit, displacement damage resulting from different irradiation sources can be compared, and irradiation-induced property changes can also be correlated. The most popular method to calculate *dpa* is a model proposed by Norgett, Robinson and Torrens [18] (NRT model), in which the number of displaced atoms produced by a PKA is given by:

$$N_d = \begin{cases} \dfrac{\kappa(T-E_e)}{2E_d} = \dfrac{\kappa T_{dam}}{2E_d}, & T_{dam} > 2E_d \\ 1, & E_d < T_{dam} < 2E_d \\ 0, & 0 < T_{dam} < E_d \end{cases} \quad (1)$$

where T is the recoil energy of a PKA, E_e is the total energy lost by electron excitation, κ is the damage efficiency, T_{dam} is the damage energy available for elastic collisions, and E_d is the threshold displacement energy averaged over all crystallographic directions. It was found that the displacement efficiency (κ) is independent of the PKA energy (except around $2E_d$) and is about 0.8 for most metals. The recoil energy T can be easily expressed in a center-of-mass system as:

$$T = \frac{2Mm}{(M+m)^2} E(1-\cos\theta) \quad (2)$$

where M and m are the masses of the impinging particle and the target atom respectively, E is the impinging particle energy, and θ is the scattering angle. Given the differential cross section of a particle of energy E to create a recoil of energy T as $d\sigma(E,T)$, the *dpa* can be obtained by:

$$dpa = \Phi \int_{E_d}^{T_{max}} N_d \frac{d\sigma(E,T)}{dT}\, dT \quad (3)$$

where Φ is the fluence, and T_{max} is the maximum energy can be transferred.

Following the initial elastic collision phase, the point defects resulting from cascade damage migrate towards various defect sinks (dislocations, grainboundaries, interfaces, etc.), and annihilation and aggregation of interstitials and vacancies take place. The typical time and energy scales of this cooling phase are in the ranges appreciable to the traditional rate theory. Thus, the kinetics of point defects clustering and microstructural evolution can be characterized by the continuity equations: [19]

$$\begin{aligned} \nabla\left(D_v \nabla C_v + \frac{D_v C_v}{kT}\nabla U_v\right) + G_v - RC_vC_i - K_vC_v &= \frac{\partial C_v}{\partial t} \\ \nabla\left(D_i \nabla C_i + \frac{D_i C_i}{kT}\nabla U_i\right) + G_i - RC_vC_i - K_iC_i &= \frac{\partial C_i}{\partial t} \end{aligned} \quad (4)$$

where v and i denote vacancies and interstitials respectively. $C_{v,i}$ are the concentrations of point defects, R is the coefficient of point defect recombination, and $K_{v,i}$ is the reaction rate constant, which is defined as the product of sink strength $S_{v,i}$ and diffusion coefficient $D_{v,i}$. $U_{v,i}$ are the interaction energies of point defects with sinks, and $G_{v,i}$ are the effec-

tive point defect generation rates that account point defects both from displacement and from sinks by thermal emission. The difference in sink strength, that is the sink capture efficiency for point defects, gives rise to a biased partition of surviving point defects among different types of sinks. As a result, irradiated microstructure evolves with these unbalanced excess fluxes of point defects at irradiation temperatures, leading to various irradiation effects, such as void swelling, irradiation creep, radiation-induced segregation, etc.

3. IRRADIATION INDUCED MICROSTRUCTURAL AND MICROCHEMICAL CHANGES IN HT-9

3.1 Dislocation Loops

Transmission electron microscope (TEM) is the most common tool used to characterize irradiation defects in structural materials. Limited by the resolution of TEM, irradiation defect clusters less than 1 to 2 nm are difficult to resolve even with the best quality TEM foils.[20] The smallest visible damage structure under TEM in martensitic steels appears as small black or white dots depending on the imaging condition. For irradiated iron-based bcc materials, interstitial dislocation loops with Burgers vectors of a/2<111> and a<100> are often observed.[21] Defects larger than 5 nm in the HT-9 steel can be identified as dislocation loops or second-phase particles. In a neutron irradiation study conducted at the High Flux Isotope Reactor (HFIR), Hashimoto et al. [22] reported that the mean diameters of a<100> and a/2<111> loops were 14 nm and 10 nm, respectively, at 400°C and 7.4 dpa. The density of a<100> dislocation loops was about $1x10^{22}$ m^{-3} and was a factor of three higher than that of a/2<111> loops. To simulate the high helium production in fusion reactors, the HT-9 steel doped with ^{58}Ni and ^{60}Ni were also investigated in this study. A slightly higher loop density was obtained in the specimens doped with ^{58}Ni. This was attributed to a higher helium production during irradiation which facilitated the nucleation of dislocation loops in the HT-9 steel. With the increase of irradiation dose and temperature, the average size of dislocation loops increases.

Dislocation microstructural study was also performed with fast neutron spectra on the HT-9 steel. The specimens were irradiated in the Materials Open Test Assembly (MOTA) of the FFTF at 420°C up to 35 dpa.[23] The size of dislocation loops observed was about 100 nm and the loop density was about $5x10^{20}$ m^{-3}. In another fast neutron irradiation study carried out at Phenix fast breeder reactor, [8] Dubuisson et al. observed a high density of dislocation loops in a group of high-Cr ferritic/martensitic steels, including HT-9, irradiated to ~100 dpa. Although no quantitative measurements were reported in the study, it was found that the dislocation structure became unstable above 500°C in high-Cr martensitic steels and the dislocation density reduced rapidly with increasing irradiation temperature. More recently, Sencer et al. [24] examined the HT-9 fuel assembly duct material irradiated in FFTF at 443°C to 155 dpa. They found the network dislocation density was about $3x10^{15}$ m^{-2}. The majority of network dislocations were a/2<111> type, and a<100> type were about 1/4 of the total population. The density of dislocation loops (predominant a<100> type) was $5x10^{20}$ m^{-3} and the mean size was about 18 nm.

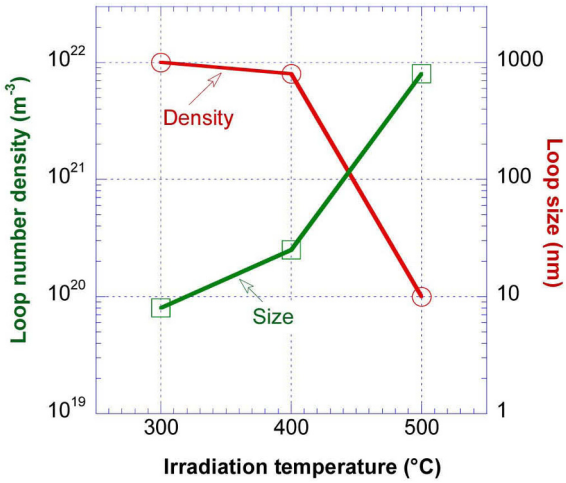

Fig. 1. Number Density and Average Diameter of Dislocation Loops Versus Irradiation Temperature for the HT-9 Martensitic Steel Irradiated by 14 MeV Nickel Ions (after Kai and Kulcinshi [25])

Irradiation induced dislocation structure was also reported in several researches with ion irradiations on the HT-9 steel. In a study conducted by Kai and Kulcinshi,[25] the HT-9 steel was irradiated using 14 MeV nickel ions up to a fluence of $8x10^{20}$ ions/cm^2. The post-irradiation TEM observation at the 40-dpa area of the specimen showed that the pre-existing dislocations in tempered martensite structure were replaced by dislocation loops. Most of the dislocation loops were identified as intestinal a<100> type. The loop density and loop size varied with irradiation temperature as shown in Fig. 1. Above 600°C, no difference can be observed between the irradiated and unirradiated regions, suggesting a recovery stage at this temperature. This temperature dependent behavior can also be seen in another "dual-beam" ion irradiation study carried out by Gilbon and Rivera.[4] In this study, 500 keV iron irradiation was performed along with helium injection. At ~100 dpa and 500°C, the network dislocation density was about $4x10^{14}$ m^{-2} similar to that in tempered high-Cr martensitic steels. The study showed that a significant recovery started to occur in the HT-9 steel at about 550°C.

3.2 Radiation-induced Segregation and Precipitation

Irradiation-induced transport processes involve two basic mechanisms: ballistic transport (i.e. atomic mixing) and radiation-enhanced diffusion. In a multiphase system, pre-existing precipitates could be dissolved by ballistic

transport during irradiation, but can also be coarsened by radiation-enhanced diffusion.[26] While the ballistic transport depends on the energy density transferred to PKAs, the radiation-enhanced diffusion is correlated well with displacement rate and irradiation temperature. Along with the flow of point defects towards the sinks, the flux of defect-solute complexes gives rise to the diffusion of alloy constituents. The difference in the diffusion rates by vacancy or interstitial mechanisms leads to an enrichment of fast moving species near sinks. This phenomenon is termed inverse Kirkendall effect and is of critical importance of radiation-induced segregation (RIS).[27] At a given damage rate, the inverse Kirkendall effect peaks around an intermediate irradiation temperature. If the irradiation temperatures are too low, a low vacancy mobility will result in high defect recombination rates. At high irradiation temperatures, the recombination rates are also high because of the enhanced back diffusion of solutes. Thus, the RIS is only effective at an intermediate temperature range where defect recombination rates are minimum. This minimum is understandably a function of damage rate and shifts toward lower temperatures with reducing damage rates. Therefore, irradiation temperature and dose rate are coupled experimental variables, and the effective ranges of RIS can be shown schematically in Fig. 2.[27]

Radiation-induced segregation of alloy elements at grainboundaries in austenitic alloys is well understood with the inverse Kirkendall mechanism. Cr depletion and Ni enrichment are widely observed in austenitic Fe-Cr-Ni systems after neutron irradiation. In ferritic/martensitic Fe-Cr alloys, however, the results of RIS are inconsistent, and Cr can be either enriched or depleted at grainboundaries. In a study of proton irradiation at 400°C, Cr enrichment was found at 3 dpa, but depletion at 7 and 10 dpa.[28] Complicated interactions between point defects and Cr are

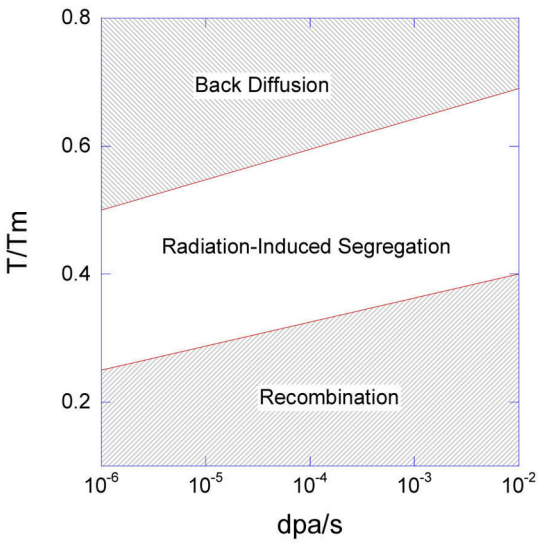

Fig. 2. Temperature and Damage Rate for Radiation-induced Segregation (after Okamoto and Rehn [27])

believed to contribute to this inconsistency.[29] Was et al. [28] showed that due to interstitial-vacancy recombination, Cr depletion would be anticipated at high temperatures for the HT-9 steel.

Radiation-induced segregations play a significant role in the formation and stability of irradiation-induced phases in ferritic/martenistic steels.[30] Without irradiation, various secondary phases are present in the HT-9 steel after heat treatments or long-term exposures at elevated temperatures. Klueh and Harries provided a detail discussion on thermal precipitates in high-Cr steels in reference [31]. The most stable carbide in unirradiated high-Cr steels is $M_{23}C_6$ which usually forms at prior austenite grain and martensite lath boundaries. Small amount of MC, M_2X and η-carbide (M_6C) can also be found in some high-Cr steels. Laves and chi (χ) phases may develop by prolonged thermal aging at elevated temperatures. After irradiation, α', G-phases, η and χ phases have been reported in HT-9.[9] In a low-dose (~7 dpa) HFIR irradiation at 400 °C, [22] Cr-rich α' and η were identified along with the dislocation loops in HT-9. The authors suggested that dislocation loops provided sites of Cr segregation and therefore played an important role in the precipitation development in martensitic steels. It is believed that the formation of α' is due to radiation-enhanced spinodal decomposition of Fe-Cr alloys,[8] and η precipitation is attributed to radiation-induced segregation of Ni and Si.[30]

In another HFIR irradiation, it was found that the original precipitate structure in HT-9 was coarsening considerably at 500°C, and the as-tempered $M_{23}C_6$ was replaced by irradiated-produced η phase.[32] Fine MC precipitates evolved and coarsened during irradiation at 300 and 500°C. Occasionally, fine G-phase particles were also reported. In contrast to this HFIR irradiation, another irradiation in the FFTF at 420°C did not alter the size and density of pre-existing $M_{23}C_6$ in the HT-9 steel considerably. Instead, fine α'(~5 nm) and χ (~13 nm) phases were identified at 35 dpa.[23] Precipitate microstructure in HT-9 was also studied in a Phenix irradiation up to 110 dpa below 530°C.[8] Apparently, the original $M_{23}C_6$ and MC were not affected by irradiation in this study. Again, new fine precipitates (η-carbide) were induced by the irradiation. These precipitates were uniformly distributed at low temperature (420°C) and narrow denuded zones could be seen along lath and grain boundaries. At 460°C, the precipitates coarsened and denuded zones widen and larger particles were produced along dislocation lines. More recently, Sencer et al. [24] and Anderoglu et al. [33] examined an HT-9 duct after long-term exposure at FFTF up to 155 dpa between 380 and 460°C. A high density of α' and G-phase precipitates were observed. The precipitation was more sensitive to the irradiation temperature than neutron dose.

Radiation induced precipitation was also reported in an irradiation conducted at the Experimental Breeder Reactor II (EBR-II) [34] and some ion irradiation studies [25]. Klueh and Harries [31] reviewed a large amount of

Table 1. Major Radiation-induced Precipitation in HT-9 (after [31]).

Irradiation Facility	Precipitate	Temperature (°C)	Dose (dpa)	Reference
FFTF	α', χ	420	35	23
	η	407	47	35
	α', G	380–440	20–155	24, 33
Phenix	α'	400–530	30–116	8
	η	419	79	8
EBR-II	α', χ, G	400, 425	25–60	34
HFIR	α', η	400	7.4	22
	G	300, 400, 500	10–12, 38	34,35
14 MeV Ni	α', χ	300–600	200	25

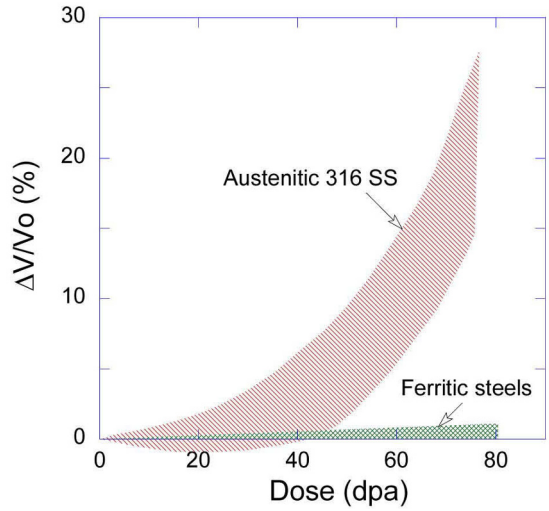

Fig. 3. Schematic of the Swelling Behavior of Ferritic/martensitic Steels vs. 316 Stainless Steel Irradiated in EBR-II at 420°C. (after Klueh [9])

work on precipitates in various high-Cr ferritic/martensitic steels. Table 1 summarizes the information concerning HT-9.

3.3 Void Swelling

Void swelling is another irradiation effect resulting from irradiation microstructural evolution. The interactions between point defects and dislocations provide the fundamental driving force of void nucleation and growth. It is well accepted that elastic interactions between interstitials and dislocations are stronger than those between vacancies and dislocations.[36] This difference is due to a relatively larger strain field surrounding a self-interstitial than a vacancy. A biased attraction between interstitials and dislocation loops leads to a preferential flux of interstitials toward dislocations.[37] Subsequently, excess vacancies become supersaturated, and void nucleation and growth take place at temperatures between 0.3-0.5 T_m.[38] Significant volumetric dilation can be observed in austenitic stainless steels and increases with irradiation dose. After an initial incubation period of slow swelling rate, a constant swelling rate about 1%/dpa can be achieved in a wide range of austenitic stainless steels independent of irradiation temperature. In contract, much less void swelling can be observed in ferritic /martensitic steels after neutron exposure. The superior swelling resistance is one of the most important advantages of ferritic/martensitic steels for nuclear applications. As shown in Fig. 3, very little volumetric change can be detected in ferritic/martensitic steels compared to austenitic stainless steels after extended neutron exposure.

The void swelling behavior of HT-9 has been reported in many neutron and ion irradiation studies. Hashimoto et al. [22] showed no void formation in standard and Ni-doped HT-9 steels irradiated in HFIR at 400°C and 7.4 dpa. Dubuisson et al. [8] also reported there was no void in HT-9 irradiated in Phenix up to 110 dpa below 530°C. No voids were observed in the HT-9 steel irradiated to 70 dpa in EBR-II. Toloczko and Garner [39] examined two heats of HT-9 irradiated in FFTF at 400 °C, and they found that only after 90-100 dpa, the two heats began to swell at relatively small but constant rates of 0.01%/dpa and 0.002%/dpa, respectively. At 165 dpa, the maximum swelling of the two heats reached 0.9%. In a dual beam ion irradiation (He^+/Fe^+) at 500°C to 100 dpa,[4] both bubbles and voids were observed in the HT-9 steel with average sizes of 2.6 nm and 8.1 nm, respectively. The calculated swelling was about 0.056%. In a recent study by Anderoglu et al. [33] on an HT-9 duct material irradiated at FFTF, voids were observed in two regions, 100 dpa at 410°C, and 155 dpa at 440°C. The calculated void swelling was 0.02% and 0.3% for 100-dpa and 155-dpa regions, respectively. No void, however, was detected at a higher irradiation temperature (466°C) at 96 dpa.

Nearly all experimental results show that the incubation period of void swelling for HT-9 is over 100 dpa, and the steady-state swelling rate is less than 0.1%/dpa. Despite the generally observed low swelling rate of HT-9, Garner et al. [40] pointed out that the steady state swelling rate of ferritic/martensitic steels may reach as high as 0.2%/dpa. The onset of swelling can also be accelerated significantly by applied stress. [39-42] Even with the highest swelling observed to date, [41] the swelling rates of HT-9 and other ferritic/martensitic steels are still considerably lower than that of austenitic stainless steels. The excellent swelling resistance of HT-9 and other ferritic /martensitic steels can be attributed to their bcc crystal structure and complicated defect-sink interactions. The proposed mechanisms responsible for the good swelling resistance of ferritic/martensitic steels summarized by Klueh and Harries [31] are: (1) solute trapping caused by weak interactions between Cr and vacancies, (2) the char-

acter of dislocation loop structure, (3) a lower dislocation bias related to bcc structure, and (4) the extensive subgrain and lath boundaries in tempered martensite microstructure. In addition, a high density of second phase precipitates (thermal or irradiation-induced) may also help suppress the void swelling. The interfaces of these particles can serve as point defect sinks which further enhance recombination in ferritic /martensitic steels.

4. IRRADIATION INDUCED MECHANICAL PROPERTY CHANGES

4.1 Tensile Properties

Tensile properties of ferritic/martenistic alloys are strongly affected by neutron irradiation. At low irradiation temperatures (<0.3Tm), the irradiated HT-9 steel shows an increased yield strength (i.e., irradiation hardening) and reduced ductility. Figure 4 shows two typical engineering stress-strain curves of HT-9 irradiated in HFIR at 90°C and 250°C along with an unirradiated control sample. [43] While the increase in yield strength is moderate for HT-9 (less than 100%) compared with other ferritic/martensitic steels, a significant loss of ductility can be observed. The unirradiated HT-9 undergoes extensive strain hardening after yielding, and the typical uniform elongation is above 10%. At ~3 dpa, the strain hardening capability of HT-9 is retained to some extent at 250°C, but is completely absent at 90°C (see Fig. 4). The lack of strain hardening leads to an early onset of plastic instability, and the uniform elongation is virtually zero after low-temperature irradiations. Obviously, this plastic deformation behavior is of serious concern for the structural applications of HT-9 in nuclear energy systems.

Irradiation hardening at low temperatures is caused by dislocation loops and defect clusters resulting from displacement damage. Thus, the degree of hardening is expected to increase with irradiation dose but eventually saturate when defect overlapping starts to occur. Some tensile test results of HT-9 obtained from low-temperature irradiations at HFIR [43] and FFTF [44] are plotted as a function of dose in Fig. 5. While the HFIR irradiation was carried out at several temperatures between 90 and 400°C, the FFTF irradiation was performed at a narrower temperature range of 373-400°C. Despite a large scatter, the dataset clearly shows that irradiation hardening increases sharply at low doses but saturates around 10 dpa for the HT-9 steel.

The effects of neutron irradiation on the tensile properties depend on irradiation temperature. While significant hardening can be seen in low-temperature irradiations, irradiation hardening does not occur above 425°C in HT-9. As the irradiation temperature increases, the magnitude of hardening decreases, and the uniform elongation increases to about a half of the unirradiated value at 400°C. [46] The decline of radiation-induced hardening becomes more evident above 400°C, as shown in Fig. 6. Enhanced softening can occur in the temperature range between 425 and 500°C as dislocation recovery takes place. [9] Above 0.3Tm, irradiated microstructure evolves gradually with the rear-

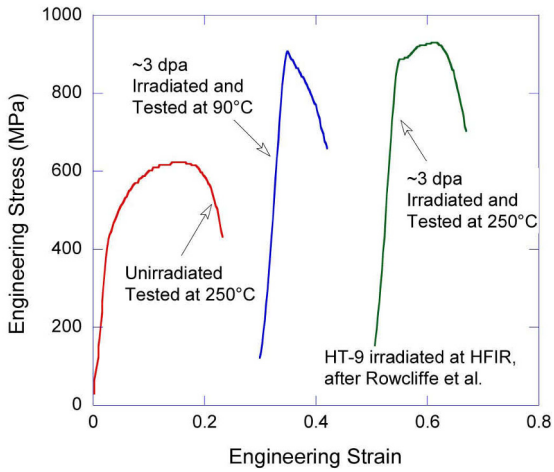

Fig. 4. Typical Engineering Stress-strain Curves of HT-9 Irradiated in HFIR at 90°C and 250°C (after Rowcliffe et al. [43])

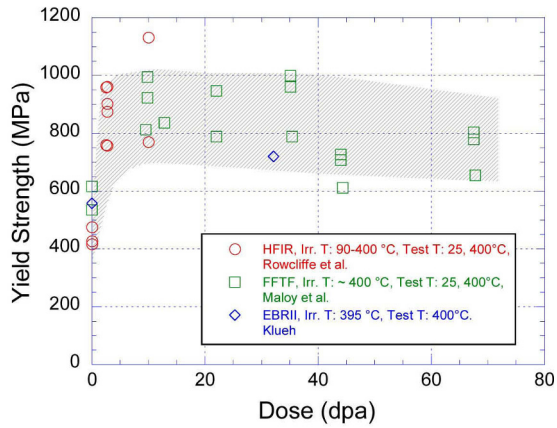

Fig. 5. Dose Dependence of Yield Strength for HT-9 Irradiated at HFIR and FFTF below 400°C. (after Rowcliffe et al. [43], Maloy et al. [44], Klueh [45])

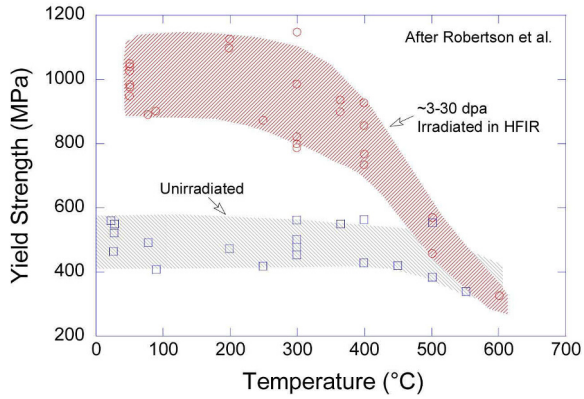

Fig. 6. Temperature Dependence of Yield Strength of HT-9 Irradiated to ~3-30 dpa (after Roberson et al. [46])

rangement of dislocations and precipitate coarsening. Irradiation enhanced diffusion and precipitation can further accelerate the microstructural evolution and thus increase the rate of softening. Beyond a certain dose, irradiation hardening vanishes at these temperatures for HT-9. The temperature sensitivity around 0.3Tm (~400°C) was demonstrated in a recent study by Maloy et al. with the HT-9 duct material irradiated in FFTF. [47] Several specimens cut from different locations of the duct were tested in compression. While a significant increase in yield strength was observed for the sample irradiated at 383°C to a dose of 28 dpa, no hardening was detected in the specimens irradiated at 443°C and 505°C to 155 and 4 dpa, respectively. It is clear that the impact of irradiation on the tensile properties is limited to temperatures below 400°C.

4.2 Irradiation Creep

Irradiation creep is a time-dependent plastic deformation phenomenon and is attributed to the supersaturation of point defects resulting from displacement damage. By altering the flux of point defects toward sinks, dislocation absorption, nucleation, climb and glide behaviors are affected by applied stresses, leading to a stress-induced microstructural evolution under irradiation. Various mechanisms have been proposed to explain irradiation creep. Since both irradiation creep and void swelling involve the redistribution of point defects during microstructural evolution, the two irradiation phenomena are coupled. Details of the theoretical treatments of irradiation creep and the correlation with void swelling are beyond this review and can be found in references [10,48-53].

The irradiation creep of HT-9 was first studied in the U. S. fast rector program in the late 1970s. [54-56] A more comprehensive irradiation creep database was established in the U. S. fusion reactor materials program in 1990s. [41, 42,57-59] The majority of irradiation creep experiments were performed in EBR-II and FFTF. Grossbeck studied the HT-9 steel in the Oak Ridge Research Reactor (ORR) and HFIR, [12,59] and another irradiation experiment by Toloczko was carried out in the Prototypic Fast Reactor (PFR). [42] The irradiation temperature ranged from 60 to 650 °C and the dose went up to 208 dpa in these tests. Table 2 summarizes the irradiation creep test conditions of these studies.

The creep deformation of HT-9 under neutron irradiation was evaluated using pressurized creep tube specimens. In a creep tube experiment, creep deformation was characterized by measuring the changes of a tube diameter before and after irradiation. The contribution of swelling was determined from measuring diametrical changes of stress-free creep tubes and destructive immersion density measurements of stressed tube specimens to examine the stress-dependence of swelling. The irradiation creep strain rate, $\dot{\varepsilon}$, can be expressed in terms of stress, σ as:

$$\dot{\varepsilon} = (B_0 + D\dot{S})\sigma^n \quad (5)$$

where B_o is the creep compliance coefficient in MPa^{-1} dpa^{-1}, D is the creep-swelling coupling coefficient, and $\dot{S}$ is the volumetric swelling rate per dpa, and n is the stress exponent, often around 1. The irradiation creep compliance coefficients, creep-swelling coupling coefficients, and swelling rates reported in the literature are also included in Table 2.

Figure 7 are representative plots showing diametrical strain as functions of irradiation dose and hoop stress of the HT-9 steel irradiated in FFTF at 403-426°C by Garner and Puigh. [7] The zero-stress curve indicates that there is a long incubation period before swelling occurs. The creep strain rate exhibits a linear relationship with stress above

Table 2. Irradiation Creep Test Conditions for HT-9.

Reactor	Irr. Temp (°C)	Dose (dpa)	Hoop Stresses (MPa)	B_0 (10^{-6} $MPa^{-1}dpa^{-1}$)	D (10^{-2} /MPa)	$\dot{S}$ (%/dpa)	Ref.
EBR-II	540-565	10-20	0 -120	3	0.3		54
EBR-II	595	10-20	0 -60				55
EBR-II	400-650	50					56
FFTF	403-426, 520	155	0-200	2.19	<1	0.015	7
FFTF	400	208	0-200	0.5	0.7-1.0	0.012	41
FFTF	400	165	0-200	0.87-1.2	0.46-1.2		39
FFTF/PFR	400	50	0-200	0.95 FFTF 1.7-1.9 PFR	0.59 FFTF		42
FFTF	400-670	50-165	0-200				57
ORR	60, 330, 400	8	0-500				12
ORR/HFIR	330	19		0.5			59

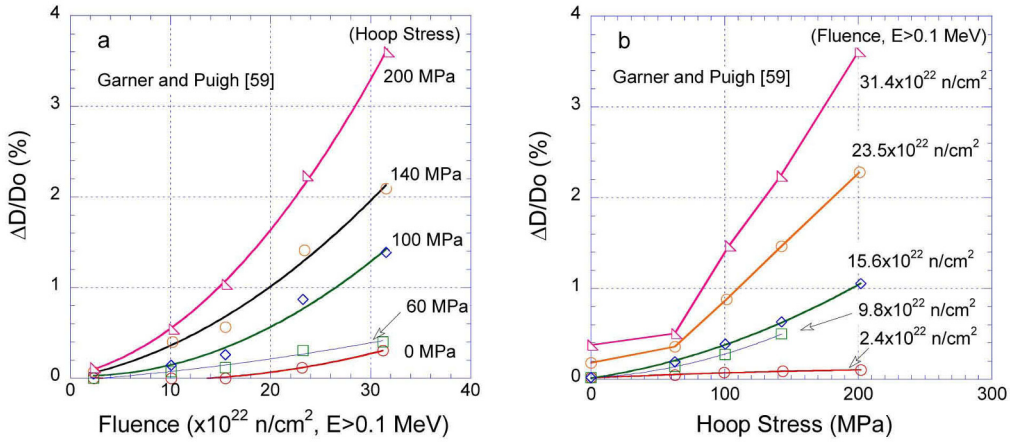

Fig. 7. Pressurized Creep Tube Tests on HT9 Irradiated in FFTF at 403-426°C (after Garner and Puigh [7]).

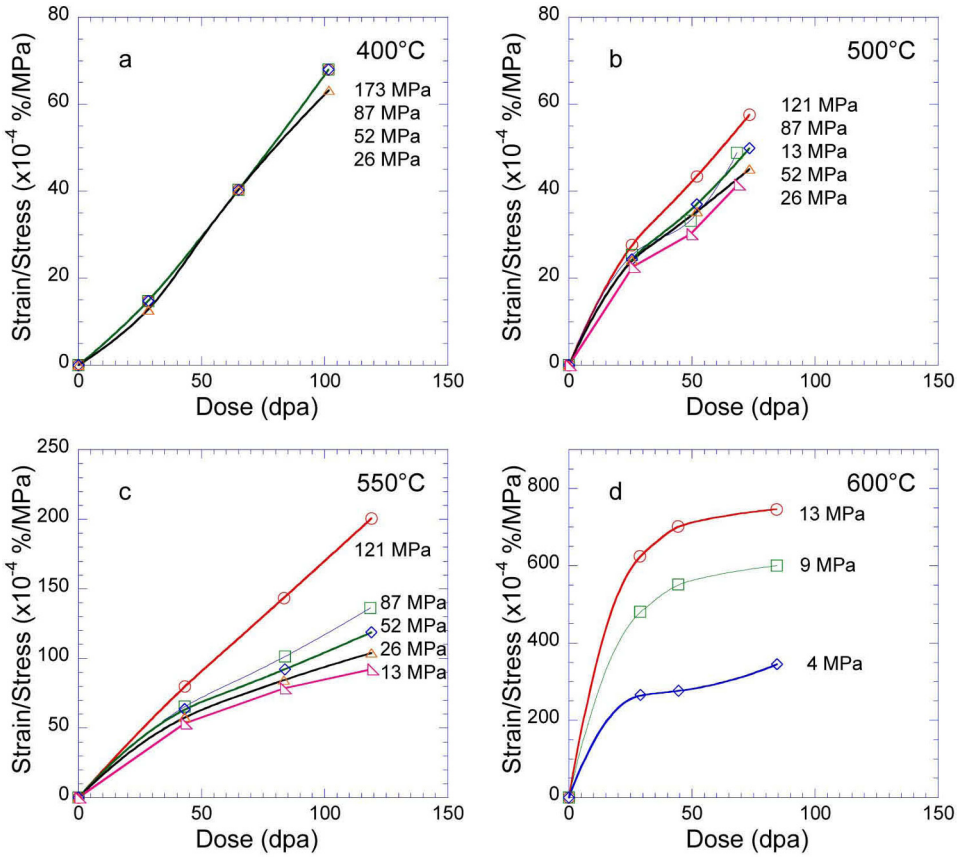

Fig. 8. A nonlinear Stress Dependence in HT9 at High Irradiation Temperature (after Toloczko et al. [58])

a hoop stress of 50 MPa at ~400 °C. At higher irradiation temperatures, a nonlinear stress dependence was observed, as shown in Fig. 8. [58] At 600°C both the creep compliance and the magnitude of the creep transient for HT-9 increased significantly, where thermal creep would be expected to dominate.

An inverse temperature effect on the irradiation creep of HT-9 was discovered by Grossbeck et al. in a low temperature irradiation. [12,59] In this work, the HT-9 steel was irradiated to 8 dpa at 60, 330 and 400 °C in the ORR. There was little difference in the creep coefficients at 330 and 400°C in agreement with previous work. However, for the specimens irradiated at 60°C, the creep rates were a factor of 6 to 18 higher than that at two higher temperatures. This inverse temperature dependence was attributed to an extended transient dose regime caused by the difference in

mobility of vacancies and interstitials at low temperatures. The excess interstitials over vacancies at lower temperatures gave rise to dislocation climb, leading to additional glide and plastic deformation. In addition, irradiation history was also found to have a strong effect on the irradiation creep and swelling behavior of HT-9. [42] The FFTF-irradiated HT-9 showed a slight positive volume change transient and the PFR-irradiated HT-9 showed a large negative volume transient. The creep compliance of PFR-irradiated HT-9 was 1.7-1.9x10^{-6} $MPa^{-1}dpa^{-1,}$ higher than typical values observed in ferritic alloys.

Based on the creep parameters of HT-9 available in the literature (Table 2), the average creep compliance is about 0.5x10^{-6} $MPa^{-1}dpa^{-1}$ before thermal creep becomes significant. This relatively low creep compliance is consistent with the fact that the irradiation creep rate of ferritic/ martenistic alloys is significantly lower than austenitic stainless steels (the creep compliance for austenitic stainless steels is in the order of ~10^{-6} $MPa^{-1}dpa^{-1}$). The creep compliance coefficient of HT-9 is found to increase with temperature above 550°C. The void swelling rate for HT-9 is about 0.012-0.015%/dpa. A recent analysis of experimental data suggests that steady state swelling rates for ferritic/martensitic steels may be as high as 0.25 to 0.5% /dpa. [40] The creep-swelling coupling coefficient D has a value of ~0.006/MPa for both austenitic and ferritic steels. The projected impact of the creep-swelling mechanism is lower (but still important) for ferritic/ martensitic steels due to their lower swelling rates compared to austenitic steels.

4.3 Fatigue

Fatigue is a material degradation developed under cyclic stress. While the general fatigue behavior of HT-9 can be found in literature, [60] very limited data are available for its fatigue response under neutron irradiation. In a study by Grossbeck et al., the HT-9 steel doped with Ni was irradiated in HFIR to 10-25 dpa at 55°C. [61] Cyclic strengthening was found in the irradiated HT-9 steel and was attributed to the helium production by transmutation. At room temperature, the cyclic hardening resulted in a slightly decline of low-cycle fatigue life of irradiated HT-9. Nevertheless, the measured fatigue life was still higher than that of the unirradiated cold-worked 316 stainless steel.

4.4 Fracture

4.4.1 Ductile-Brittle Transition Temperature

As a bcc structure alloy, HT-9 exhibits a sharp transition from ductile to brittle fracture mode at a certain temperature in impact tests. The DBTT of unirradiated HT-9 is below room temperature. However, the low-temperature irradiation embrittlement could shift this transition to a much higher temperature and reduce the upper shelf energy considerably. A comparison of unirradiated and irradiated Charpy impact test results from reference [9] is shown in Fig. 9. This low-temperature embrittlement is the greatest concern for the

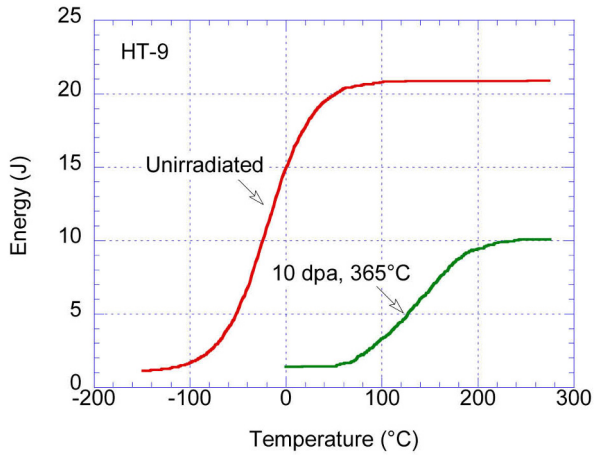

Fig. 9. Charpy Impact Test Results of HT-9 Irradiated in FFTF at 365 °C (after Klueh [9]).

applications of HT-9 in nuclear systems.

In a recent study on the FFTF fuel duct, Byun et al. [62] performed some impact tests on the HT-9 specimens sectioned from different positions. The irradiation doses and temperatures of these specimens ranged from 3 to 148 dpa and from 378 to 504°C, respectively. The measured upper-shelf energy was about 2-5 J after irradiation, significantly lower than that of unirradiated control samples. The DBTT shift was found to be insensitive to irradiation dose, suggesting a saturated behavior among these samples above 3 dpa.

The shift in DBTT for HT-9 reported in reference [2] was about 124°C after irradiations in EBR-II and FFTF to about 26 dpa at 375-390°C. This temperature shift was more than a factor of two higher than that for a modified 9Cr-1Mo alloy. A larger amount of carbides in the HT-9 steel was to blame for this considerable DBTT shift. The presence of delta ferrite can also affect the strength and toughness of high-Cr martensitic steels. These influences of pre-irradiation microstructures suggest that the normalizing-and-tempering treatment can affect the DBTT shift for the HT-9 steel.

As discussed in the section of tensile properties, radiation hardening can be offset by softening when irradiation temperature is higher than 425°C. Irradiation embrittlement is recovered to some extent thanks to a dislocation recovery process and precipitate coarsening. As a result, the shift in DBTT decreases with the increase of irradiation temperature. Byun et al. [62] showed a sharp decline in the DBTT between 400 and 450°C. However, the DBTT shift does not approach zero at high irradiation temperatures when irradiation hardening is completely absent. The remaining DBTT shift is attributed to the M_6C precipitates in HT-9. Dubuisson et al. [8] found that the temperature shift increases with density of M_6C precipitates in HT-9. At high temperatures, irradiation-induced precipitates contribute to the embrittlement of HT-9.

4.4.2 Fracture Toughness

A large body of fracture toughness data on HT-9 was produced in the EBR-II and FFTF irradiations at temperatures and neutron doses ranged from 390-600°C and 35-100 dpa, respectively. From a summary paper by Huang and Hamilton,[63] the measured J values for the irradiated specimens were slightly lower than the values for the unirradiated condition, while the tearing modulus showed a significant reduction after irradiation, especially at the lowest temperature.

As the tensile properties of HT-9 irradiated at temperatures below 250°C exhibited a significant irradiation hardening and a complete loss of uniform elongation, a low fracture toughness value is anticipated after low temperature neutron irradiation. Rowcliffe et al. [43] summarized the fracture toughness data from several sources for HT-9 irradiated to 1.5-2.5 dpa at 80-90°C and 250-300°C. The fracture toughness of unirradiated HT-9 falls in the range of 200–300 MPa $\sqrt{m}$ over the temperature range of 20 to 300°C, and the transition temperature at 100 MPa $\sqrt{m}$ for unirradiated HT-9 is about -75°C. A low-dose irradiation at ~80°C increases the K_J transition temperature for HT-9 by about 100°C, whereas an irradiation at ~300°C increases the transition temperature by about 275°C. In addition, the higher irradiation temperature results in a significant reduction in the upper shelf fracture toughness. For the test temperature of 250°C, the upper shelf regime has a K_J value of 164 MPa $\sqrt{m}$ for HT-9. At room temperature, the HT-9 steel exhibits a lower shelf behavior and a K_J of 31 MPa $\sqrt{m}$.

A recent fracture toughness J-R curve testing study conducted by Byun et al. [64] on the FFTF fuel duct confirmed the previous results on HT-9. Among the samples tested, no clear dose-dependence could be found between 3 and 148 dpa. The irradiation temperature in the range be-tween 378 and 504°C, however, had a dominant effect on the post-irradiation fracture toughness. While a fracture toughness value less than 50 MPa $\sqrt{m}$ could be seen for the specimens irradiated below 400°C, all specimens irradiated above 430°C had a fracture toughness value well above 100 MPa $\sqrt{m}$. This post upper-shelf behavior suggested that the DBTTs are below room temperature for the specimens irradiated at high temperatures.

4.4.3 High Temperature Helium Embrittlement

Helium is a transmutation product from (n, α) reaction whose cross-section is higher in thermal spectrum. The role of helium in irradiation hardening and embrittlement is a long standing question for ferritic/martensitic steels. Based on the fact that HFIR irradiation produced larger degradation in both toughness and tearing modules than that of FFTF irradiation, Huang and Hamilton [63] suggested that helium played a significant role on radiation hardening. In a recent study using a HT-9 steel doped with Ni, Klueh et al. [65,66] also observed increased hardening due to helium. It is suggested that the helium may stabilize vacancy clusters and contribute to the formation of interstitial loops. With the increase of helium content, the intergranular fracture can occur at high temperatures leading to helium embrittlement. It is believed that the helium-filled cavities or bubbles could become nuclei for fracture at elevated temperatures.

5. SUMMARY

The HT-9 martensitic steel is a promising candidate material for various advanced nuclear energy systems with high operating temperatures and severe irradiation environments. Its excellent swelling resistance and adequate high-temperature properties have been confirmed in various irradiation experiments carried out with fast and mixed spectrum reactors or ion accelerators. The adequate in-core performance of HT-9 has also been demonstrated by its successful applications as fuel cladding and ducts in FFTF. The most critical issue that may limit the usage of HT-9 in the future nuclear energy systems is its irradiation embrittlement at low temperatures. A significant shift in DBTT above 120°C can be observed after neutron irradiation below 400°C. Irradiation hardening, radiation-induced precipitation and helium production are all important factors for the low-temperature irradiation embrittlement. A satisfactory creep performance can be achieved up to 650°C with the HT-9 steel. The average creep compliance is about $0.5X10^{-6}$ MPa^{-1} dpa^{-1}, about a half of the creep compliance of austenitic stainless steels.

While the current information on the irradiation effects of HT-9 is more comprehensive than that of other ferritic /martenistic steels, the existing database is far from complete. Long-term irradiation creep data are required for the in-core applications. The current understanding on phase stability and precipitation under extreme irradiation environments needs also be improved. To address the issue of low-temperature embrittlement adequately, systemic investigations on the fracture behaviors of HT-9 are needed at a wide range of doses and temperatures relevant to the in-core conditions of advanced nuclear energy systems.

ACKNOWLEDGEMENTS

This work is supported by the U.S. Department of Energy, Office of Nuclear Energy, under contract # DE-AC02-06CH11357.

REFERENCES

[1] Kalwa, G., K. Haarmann, and J.K. Janssen, in: Topical Conference on Ferritic Alloys for Use in Nuclear Energy Technologies, Eds. J.W Davis and D.J. Michel (Met Soc. AIME, Warrendale, PA, 1984) 235.

[2] Klueh, R.L. and D.J. Alexander, "Heat treatment effects on impact toughness of 9Cr–1MoVNb and 12Cr–1MoVW steels irradiated to 100 dpa", J. Nucl. Mater., 253-258(1998)

1269-1274.
[3] Gelles, D. S., "Development of Martensitic Steels for High Neutron Damage Applications," J. Nucl. Mater., 239 (1996): 99-106.
[4] Ghoniem, N. M., J. Blink, and N. Hoffman, "Selection of alloy steel type for fusion power plant applications in the 350-500C range," Proc. of the Topical Conf. on Ferritic Alloys for Use in Nuclear Technology, Snowbird, Utah. 1983.
[5] Gilbon, D. and C. Rivera, "Behavior of different ferritic steels under ion, electron and fast neutron irradiation", J. Nucl. Mater., 155-157 (1988) pp.1268-1273
[6] Allen, T. R, J. T. Busby, R. L. Klueh, S. A. Maloy, and M. B. Toloczko, "Cladding and duct materials for advanced nuclear recycle reactors," JOM 60, no. 1 (2008): 15-23.
[7] Garner, F.A. and R.J. Puigh, "Irradiation creep and swelling of the fusion heats of PCA, HT9 and 9Cr-1Mo irradiated to high neutron fluence", J. Nucl. Mater., 179-181 (1991) 577-580.
[8] Dubuisson, P., D. Gilbon and J. L. Seran, "Microstructural evolution of ferritic-martensitic steels irradiated in the fast breeder reactor Phenix", J. Nucl. Mater., 205 (1993) 178-189
[9] Kluek, R.L., "Elevated temperature ferritic and martensitic steels and their application to future nuclear reactors", International Materials reviews, Vol. 50, No.5, 2005, pp287-310.
[10] Stiegler, J. O. and L.K. Mansur, Ann. Rev. Mater. Sci., "Radiation effects in structural materials", 1979. 9. pp.405-454
[11] Gelles, D. S., "Effects of irradiation on low activation ferritic alloys: a review," *Reduced Activation Materials for Fusion Reactors*, R. L. Klueh, D. S. Gelles, M. Okada, and N. H. Packin, Eds., Amer. Soc. for Testing and Materials, Philadelphia (1990): 113.
[12] Grossbeck, M. L., L. K. Mansur, "Low-temperature irradiation creep of fusion reactor structural materials" J. Nucl. Mater. 179-181 (1991): 130.
[13] Strang, A., and V. Vodarek, "The effects of microstructural stability on the creep properties of high temperature martensitic 12 Cr steels," 7th International Conference on Creep and Fracture of Engineering Materials and Structures, 1997.
[14] Masuyama, F., "History of power plants and progress in heat resistant steels," ISIJ internaltional, 41.6 (2001): 621-625.
[15] Robinson, M.T., "Basic physics of radiation damage production", J. Nucl. Mater., 216(1994): 1-28.
[16] Greenwood, L. R., "Neutron Interactions and Atomic Recoil Spectra," J. Nucl. Mater., 216 (1994): 29-44
[17] Averback, A.S., "Atomic displacement processes in irradiated metals", J. Nucl. Mater., 216(1994): 49-62
[18] Norgett, M.J., M.T. Robinson and I.M. Torrens, "A proposed method of calculating displacement dose rates", Nuclear Engineering and Design, 33 (1975) pp. 50-54
[19] Mansure, L.K., "Theory and experimental background on dimensional changes in irradiated alloys", 216 (1994): 97-123.
[20] Jenkins, M.L., "Characterization of radiation-damage microstructures by TEM", J. Nucl. Mater., 216 (1994):124-156
[21] Eyre, B. L., A. F. Bartlett, "An Electron Microscope Study of Neutron Irradiation Damage in Alpha-iron," Phil. Mag., 12,116 (1965):261
[22] Hashimoto, N., J. P. Robertson, and K. Shiba, "Microstructure of Isotopically-tailored Martensitic steel HT9 Irradiated at 400C to 7 dpa in HFIR," DOE/ER-0313/26 – Vol. 26, Semiannual Progress Report, June 30, 1999, pp.96-101.
[23] Kai, J.J. and R.L. Klueh, "Microstructural analysis of neutron-irradiated martensitic steels", J. Nucl. Mater., 230(1996) pp. 116-123
[24] Sencer, B.H., J.R. Kennedy, J.I. Cole, S.A. Maloy, F.A. Garner, "Microstructural analysis of an HT9 fuel assembly duct irradiated in FFTF to 155 dpa at 443°C," J. of Nucl. Mater., 393(2) (2009): 235-241.
[25] Kai, J.J. and G.L. Kulcinshi, "14 MeV nickel-ion irradiated HT-9 ferritic steel with and without helium pre-implantation", J. Nucl. Mater., 175 (1990) pp. 227-236
[26] Wollenberger, H., "Phase transformation under irradiation", J. Nucl. Mater., 216 (1994) pp. 63-77
[27] Okamoto, P.R. and L.E. Rehn, "Radiation-induced segregation in binary and ternary alloys", J. Nucl. Mater., 83 (1979) pp.2-23
[28] Was, G. S., J. P. Wharry, B. Frisbie, B. D. Wirth, D. Morgan, J. D. Tucker, and T. R. Allen, "Assessment of radiation-induced segregation mechanisms in austenitic and ferritic –martensitic alloys," Journal of Nuclear Materials 411, no. 1 (2011): 41-50.
[29] Wong, K. L., J. H. Shim, and B. D. Wirth, "Molecular dynamics simulations of point defect interactions in Fe–Cr alloys," Journal of nuclear materials 367 (2007): 276-281.
[30] Maziasz, P.J., "Formation and stability of radiation-induced phases in neutron-irradiated austenitic and ferritic steels", J. Nulc. Mater., 169 (1989) pp.95-115
[31] Klueh, R.L. and D.R. Harries, "High-Chromium Ferritic and Martensitic Steels for Nuclear Applicaitons", ASTM, West Conshohocken, PA.
[32] Maziasz, P.J., R.L. Klueh and J.M. Vitek, "Helium effects on void formation in 9Cr-1MoVNb and 12Cr-1MoVW irradiated in HFIR", J. Nucl. Mater., 141-143 (1986) pp. 929-937
[33] Anderoglu, O., J. Van den Bosch, P. Hosemann, E. Stergar, B. H. Sencer, D. Bhattacharyya, R. Dickerson, P. Dickerson, M. Hartl, and S. A. Maloy, "Phase stability of an HT-9 duct irradiated in FFTF," Journal of Nuclear Materials, 430 (2012): 194-204.
[34] Gelles, D. S., L. E. Thomas, "Effects of neutron irradiation on microstructure in experimental and commercial ferritic alloys," Ferritic Alloys for Use in Nuclear Energy Technologies, Eds, J. W. Davis, and D. J. Michel, Met. Soc. AIME, 1984, 559.
[35] Maziasz, P. J., Materials for Nuclear Reactor Core Applications, Vol. 2, British Nuclear Energy Society, 1988, 61.
[36] Hirth, J. P. and J. Lothe, *Theory of Dislocations*, 2nd Ed., Krieger Publishing Company, Malabar, Florida, 1992.
[37] Heald, P. T., "Preferential Trapping of Interstitials at Dislocations," Phil. Mag., **31**, 3 (1975) 551.
[38] Gittus, J., Irradiation effects in crystalline solids, Applied Science Publishers LTD., London, 1978.
[39] Toloczko, M.B. and F.A. Garner, "Irradiation creep and void swelling of two LMR heats of HT9 at ~400°C and 165 dpa", J. Nucl. Mater., 233-237 (1996) 289-292.
[40] Garner, F. A., M. B. Toloczko, B. H. Sencer, "Comparison of swelling and irradiation creep behavior of fcc-austenitic and bcc-ferritic/martensitic alloys at high neutron exposure",

J. Nucl. Mater. 276 (2000) 123.
[41] Toloczko, M. B., F. A. Garner, C. R. Eiholzer, "Irradiation creep and swelling of the US fusion heats of HT9 and 9Cr-1Mo to 208 dpa at ~400°C" J. Nucl. Mater. 212-215 (1994) 604.
[42] Toloczko, M. B., F. A. Garner, C. R. Eiholzer, "Irradiation creep of various ferritic alloys irradiated at ~400°C in the PFR and FFTF reactors" J. Nucl. Mater. 258-263 (1998) 1163.
[43] Rowcliffe, A.F., J.P. Robertson, R.L. Klueh, K. Shiba, D. J. Alexander, M. L. Grossbeck and S. Jitsukawa, "Fracture toughness and tensile behavior of ferritic–martensitic steels irradiated at low temperatures", J. Nucl. Mater. 258-263 (1998) 1275.
[44] Maloy, S.A., M. B. Tolocako, K.J. McClellan, T. Romero, Y. Kohno, F.A. Garner, R.J. Kurtz and A. Kimura, "The effects of fast reactor irradiation conditions on the tensile properties of two ferritic/martensitic steels", J. Nucl. Mater. 356 (2006) 62.
[45] Klueh, R. L., "Irradiation Effects on Tensile Properties of High-Chromium Ferritic/Martensitic Steels," DOE/ER-0313/35 – Vol. 35, Semiannual Progress Report, Dec. 31, 2003, pp.73-79.
[46] Robertson, J.P., R.L. Klueh, K. Shiba and A.F. Rowcliffe, "Radiation hardening and deformation behavior of irradiated ferritic-martensitic Cr-steels", in Fusion Materials Semi ann. Prog. Report for period ending Dec. 31 1997, DOE/ER-0313/23, Oak Ridge National Lab, 1997, pp. 179-187.
[47] Maloy, S. A., M. Toloczko, J. Cole, T. S. Byun, "Core materials development for the fue cycle R&D program," J. Nucl. Mater. 415 (2011) 302-305.
[48] Bullough, R., and M.R. Hayns, "The temperature dependence of irradiation creep," J. Nucl. Mater., 65 (1977): 184-191
[49] Wolfer, W. G., "Correlation of radiation creep theory with experimental evidence," J. Nucl. Mater., 90 (1980): 175-192
[50] Woo, C. H., and F.A. Garner, "A SIPA-based theory of irradiation creep in the low swelling rate regime," J. Nucl. Mater., 191–194 (1992): 1309-1312.
[51] Woo, C. H., B.N. Singh, and A.A. Semenov, "Recent advances in the understanding of damage production and its consequences on void swelling, irradiation creep and growth," J. Nucl. Mater., 239 (1996): 7-23.
[52] Boltax, A., J.P. Foster, R.A. Weiner, A. Biancheria, "Void swelling and irradiation creep relationships," J. Nucl. Mater., 65(1977): 174-183
[53] Garner, F. A., "Irradiation Performance of Cladding and Structural Steels in Liquid Metal Reactors," *Materials Science and Technology – A Comprehensive Treatment*, Ed. R.W. Cahn, P. Haasen, E. J. Kramer, 1994.
[54] Paxton, M. M., B. A. Chin, E. R. Gilbert, R. E. Nygren, "Comparison of the in-reactor creep of selected ferritic, solid solution strengthened, and precipitation hardened commercial alloys", J. Nucl. Mater. 80 (1979) 144.
[55] Paxton, M. M., B. A. Chin, E. R. Gilbert, "The in-reactor creep of selected ferritic, solid solution strengthened, and precipitation hardened alloys", J. Nucl. Mater. 95 (1980) 185.
[56] Chin, B. A., in Topical Conference on Ferritic Steels for Use in Nuclear Energy Technologies, Eds. J. W. Davis, D. J. Michel (The Metallurgical Society of AIME, Warrendale, PA, 1984) 593.
[57] Toloczko, M. B., F. A. Garner, "Stress and temperature dependence of irradiation creep of selected FCC and BCC steels at low swelling" Fusion Materials Program Semiannula Progress Report, (2002) p. 73.
[58] Toloczko, M. B., D. S. Gelles, F. A. Garner, R. J. Kurtz, K. Abe, "Irradiation creep and swelling from 400 to 600°C of the oxide dispersion strengthened ferritic alloy MA957", J. Nucl. Mater. 329-333 (2004) 352.
[59] Grossbeck, M. L., L. T. Gibson, S. Jitsukawa, "Irradiation creep in austenitic and ferritic steels irradiated in a tailored neutron spectrum to induce fusion reactor levels of helium"J. Nucl. Mater. 233-237 (1996) 148.
[60] James, L. A., "Fatigue-Crack Propagation Behavior of HT-9 Steel," *J. Nucl. Mater*., 149(1987):138-142.
[61] Grossbeck, M. L., Vitek, J. M., and Liu, K. C., "Fatigue Behavior of Irradiated Helium-Containing Ferritic Steels for Fusion Reactor Applications" *J. Nucl. Mater*., Vol. 141-143, 1986, pp. 966-972.
[62] Byun, T. S., W. Ds. Lewis, M. B. Toloczko, S. A. Maloy, "Impact properties of irradiated HT9 from the fuel duct of FFTF," J. Nucl. Mater., 421(2012):104:111.
[63] Huang, F. and M. L. Hamilton, "The fracture toughness database of ferritic alloys irradiated to very high neutron exposure", J. Nucl. Mater. 187 (1992) 278
[64] Byun, T. S., M. B. Toloczko, T. A. Saleh, S. A. Maloy, "Irradiation dose and temperature dependence of fracture toughness in high dose HT9 steel from the fuel duct of FFTF," J. Nucl. Mater., 432(2013): 1-8.
[65] Klueh, R.L., N. Hashimoto, M.A., Sokolov, K. Shiba, S. Jitsukawa, "Mechanical properties of neutron-irradiated nickel-containing martensitic steels: I. Experimental study", 357 (2006) 156-168.
[66] Klueh, R.L., N. Hashimoto, M.A., Sokolov, P.J. Maziasz, K. Shiba, S. Jitsukawa, "Mechanical properties of neutron-irradiated nickel-containing martensitic steels: II. Review and analysis of helium-effect studies", J. Nucl. Mater, 357 (2006) 169-182.